The phase transitions of ferroelastic K2SeBr6: A calorimetric and x-ray diffraction study

Walter Abriel and Mary Anne White

Citation: The Journal of Chemical Physics **93**, 8321 (1990); doi: 10.1063/1.459315
View online: http://dx.doi.org/10.1063/1.459315
View Table of Contents: http://scitation.aip.org/content/aip/journal/jcp/93/11?ver=pdfcov
Published by the AIP Publishing

The phase transitions of ferroelastic K_2SeBr_6: A calorimetric and x-ray diffraction study

Walter Abriel
Institut für Anorganische Chemie der Universität, P.O. Box 397, D-8400 Regensburg, Federal Republic of Germany

Mary Anne White
Department of Chemistry, Dalhousie University, Halifax, Nova Scotia B3H 4J3, Canada

(Received 29 September 1989; accepted 16 August 1990)

Guinier x-ray powder diffraction data in the temperature range from $T = 10$ to 290 K, and heat capacity measurements from $T = 40$ to 280 K indicate three phases for K_2SeBr_6. The high-temperature cubic structure [K_2PtCl_6-type, space group $Fm\bar{3}m$; $a = 10.4211(7)$ Å at $T = 290$ K] transforms at 237.8 ± 0.3 K with $\Delta S_{tr} = (1.36 \pm 0.02)$ J K^{-1} mol^{-1} to a tetragonal phase with a Rb_2TeI_6-type structure [space group $P4/mnc$; $a = 7.313(1)$ Å, $c = 10.474(2)$ Å at $T = 220$ K]. A second phase transition at 215 ± 1 K [$\Delta S_{tr} = (0.54 \pm 0.01)$ J K^{-1} mol^{-1}] results in a monoclinic phase with a K_2TeBr_6-type structure [space group $P2_1/n$; $a = 7.265(3)$ Å, $b = 7.265(3)$ Å, $c = 10.438(4)$ Å, $\beta = 89.66(5)°$ at $T = 80$ K]. Both transitions can be interpreted in terms of softening of rotary phonons at the X edge of the Brillouin zone. From the thermal parameters of a single crystal x-ray structure determination at $T = 293$ K, this low-temperature instability can be predicted. The results agree with comparable data of ferroelastic K_2TeBr_6 and refute some earlier speculations concerning the phase transitions in K_2SeBr_6.

I. INTRODUCTION

The great current interest in compounds with hexahalogenated complex anions of the tetravalent elements Se and Te is due to two different aspects.

In 1957, Gillespie and Nyholm[1] predicted that hexacoordinated complexes of Se(IV) and Te(IV) should not possess regular octahedral structures, but rather have structures based on seven-coordination, with a lone pair of electrons occupying the seventh position. However, the crystal structures of their alkali salts, for example K_2TeBr_6,[2] indicated that such complexes are in fact regular octahedra. Consequently, these AX_6E species (E = lone pair of electrons) were considered to be exceptions to the valence shell electron pair repulsion (VSEPR) rules.[3]

More recent papers distinguish between dynamically distorted species ("regular octahedra") and statically distorted species with respect to the symmetry of the crystal field and its influence on the phonon–electron (vibronic) coupling.[4–6] For compounds A_2SeX_6 and A_2TeY_6 (with $A = K^+$, NH_4^+, Rb^+, Cs^+; $X = Cl^-$, Br^-; $Y = Cl^-$, Br^-, I^-), the high-temperature phases show the cubic K_2PtCl_6-type structure (Fig. 1).[5,7,8] Lowering the temperature usually produces second-order phase transformations, especially when the anions are comparatively large. These phase transitions can be described by a softening of the rotary phonons. Generally, in A_2MX_6 compounds this instability is the result of a double minimum in the Coulomb potential with respect to the octahedral tilt angle ϕ around [001]; the depth of this minimum depends on the interaction strength and the radii of the corresponding ions.[9]

The second-order phase transitions of the simple alkali-hexahalogenotellurates (IV) yield ferrorotative distorted (space group $I4/m$) or antiferrorotative distorted (space groups $P4/mnc$ and $P2_1/n$) structures exclusively.[8] As the phonon structure of the alkali-hexahalogenoselenates (IV) should be of the same type, one should observe similar phase transitions for K_2SeBr_6, for example. Due to the ionic radii ratios, a symmetry reduction along the antiferrorotative path of the group–subgroup symmetry tree[8] is expected for this compound. However, papers of Nakamura *et al.*,[10] reporting an NQR study, and of Noda *et al.*,[11] giving results of an x-ray single crystal investigation, contradict this anticipation. These authors found three phase transitions (at

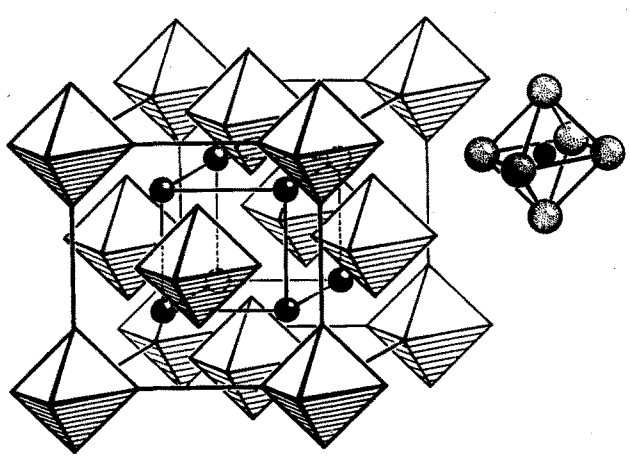

FIG. 1. K_2PtCl_6 structure. Small spheres are K, octahedra are $PtCl_6$ ($SeBr_6$).

 0021-9606/90/238321-07$03.00

$T = 212, 221$, and 238 K), with the extra intermediate phase with monoclinic symmetry and space group $C2/n$.

This puzzling situation induced us to reinvestigate K_2SeBr_6 using recently developed x-ray powder diffraction equipment for the highest possible θ resolution, complemented by calorimetric measurements. The x-ray and calorimetric experiments were carried out from ambient temperatures down to 10 and 40 K, respectively. In addition, single crystal x-ray work at 293 K was carried out to improve the early results of Hoard and Dickinson[12] with an accurate determination of the displacement parameters.

II. EXPERIMENTAL

A. Preparation

Deep red crystals of K_2SeBr_6 were precipitated from an equimolar solution of SeO_2 and KBr in concentrated hydrobromic acid. A single crystal with faces {100} and {111} and a volume of 2.64×10^{-3} mm^3 was sealed in a glass capillary. Powder with particle size less than 50 μm was prepared by crushing single crystals; this was sieved onto a silicone-moistened 0.02 mm thick aluminized Mylar foil on the sample holder of the powder diffractometer.

B. Single crystal x-ray diffraction

The single crystal data collection at 293 K was performed with a SIEMENS AED2 diffractometer using graphite-monochromatized MoKα-radiation. The cell parameter was determined from 17 reflections in the θ range 7°–18°: cubic system, F centered with $a = 10.4224(6)$ Å. Intensity data collection: maximum $\sin\theta/\lambda = 0.644$ Å^{-1}; range of hkl $-13, -13, -13$ to 13,13,13, in ω-scan mode (minimum scan angle 1.2°, maximum scan time 24 s); reflections 222, $\bar{2}2\bar{2}$, and $2\bar{2}2$ were used for standard intensity measurements; intensity variation was less than 2%. 2897 measured reflections yielded 95 unique reflections of which 88 reflections with $F > 3\sigma(F)$ were considered as observed ($R_{int} = 0.12$). (This rather poor R_{int} is probably the result of anisotropic extinction effects which also have been observed in other crystals of this structure type.[2]) Numerical absorption correction ($\mu = 246.6$ cm^{-1}) was applied with a min/max transmission of 0.059/0.141. With the structure model of Hoard and Dickinson,[12] the refinement of six parameters in the space group $Fm\bar{3}m$ using 88 F values resulted in a final $R = 0.0562$, $wR = 0.0355$ with $w = 1/\sigma^2(F)$ and $S = 5.85$ (see Ref. 13 for definitions); maximum shift/esd = 0 in the last cycle of the refinement; $1 \geqslant \Delta \geqslant -2.1$ from the final ΔF synthesis. Neutral atom scattering factors were taken from International Tables.[14] The program used was STRUCSY from the diffractometer software package. (Lists of observed and calculated structure factors and crystal dimensions and absorption corrections range are deposited in PAPS.[14])

C. X-ray powder diffraction

The x-ray powder diffraction pattern was recorded with a recently developed Guinier diffractometer, using Ge-monochromatized CuKα_1 radiation. The temperature was varied from 10 to 290 K, and was maintained with a closed-cycle helium refrigerator. The temperature was measured to ± 2 K with a silicon diode sensor in intimate contact with the sample holder. Typical parameters for a diagram recording were a step width of 0.01° and a counter time of at least 4 s per step in the range $5° \leqslant \theta \leqslant 50°$. The whole temperature range was scanned in steps of 14 K, and around the critical temperatures additional diagrams were recorded in steps of 2 K. To investigate the order of the transitions, measurements were taken with increasing and decreasing temperature. A detailed description of the set-up is given elsewhere.[15]

TABLE I. Final structural parameters for K_2SeBr_6 at $T = 293$ K, space-group $Fm\bar{3}m$, $U = \exp[-2\pi^2(aU_{11}h^2 + bU_{22}k^2 + cU_{33}l^2)]$.

Se in 4a (0,0,0)	$U_{11} = 0.022(1)$
Br in 24e (x,0,0)	$x = 0.2451(1)$
	$U_{11} = 0.0205$
	$U_{22} = U_{33} = 0.077(1)$
K in 8c (1/4, 1/4, 1/4)	$U_{11} = 0.065(2)$

D. Calorimetry

The heat capacity of a 4.107 g sample of K_2SeBr_6 was measured from $T = 39$ to 280 K. The calorimetric measurements were carried out by the adiabatic heat-pulse method; the set-up is described in detail elsewhere.[16,17] Briefly, this method involves the measurement of the absolute value of the total heat capacity of the sample and the sealed calorimetric vessel through the determination of the temperature increase in response to a quantified (Joule heating) energy, while maintaining adiabatic conditions. Through knowledge of the predetermined heat capacity of the empty sample vessel as a function of temperature, the heat capacity of the sample is calculated. Previous measurements of the heat capacity of Calorimetry Conference (NBS-49) benzoic acid agreed with the literature values[18] to within 0.5% for this calorimeter.[17]

III. RESULTS

For K_2SeBr_6 at 293 K, the K_2PtCl_6 structure was confirmed with the final structural parameters given in Table I. The interatomic distances are given in Table II. A subsequent correction of the positional parameter of the Br atom was applied because of the shortening of the Se–Br bond due to thermal motion;[19] this correction assumed that the rigid $SeBr_6^{2-}$ ion is librating about the central Se atom. The corrected atomic Se–Br distance is 2.575(2) Å, in very good agreement with the corresponding value from the structure

TABLE II. Interatomic distances (in Å, uncorrected) for K_2SeBr_6 at $T = 293$ K.

Se–Br	(6x)	2.555(1)
Br–Br	(4x)	3.613(1)[a]
Br–Br	(4x)	3.756(1)[b]
K–Br	(12x)	3.685(1)

[a] Within anion.
[b] Between anions.

TABLE III. Lattice parameters from $T = 290$ K to 10 K for K_2SeBr_6. For better comparison, the volume of the cubic cell was divided by 2.

T/K	a/Å	b/Å	c/Å	β[a]/deg	V/Å^3	Number of reflections used for refinement
290	10.4211(7)				565.9(1)	23
276	10.4144(8)				564.8(1)	23
262	10.4067(6)				563.5(1)	25
248	10.4004(6)				562.5(1)	25
234	7.327(1)		10.458(2)		561.5(1)	29
220	7.313(1)		10.474(2)		560.2(1)	26
206[b]	7.3070(8)		10.478(1)		559.4(1)	30
192	7.301(2)	7.304(3)	10.481(4)	89.90(4)	558.9(2)	10
178	7.296(3)	7.298(3)	10.476(4)	89.87(3)	557.8(3)	10
164	7.288(2)	7.294(3)	10.472(3)	89.81(4)	556.6(2)	10
150	7.287(4)	7.287(4)	10.472(6)	89.80(6)	556.1(4)	10
136	7.282(3)	7.285(3)	10.464(4)	89.78(4)	555.1(3)	10
122	7.277(2)	7.280(3)	10.461(4)	89.78(4)	554.2(3)	10
108	7.273(3)	7.275(3)	10.451(4)	89.70(4)	553.0(3)	10
94	7.268(2)	7.269(2)	10.446(3)	89.66(3)	551.8(2)	10
80	7.265(3)	7.265(3)	10.438(4)	89.66(5)	550.9(3)	10
66	7.264(3)	7.263(4)	10.435(5)	89.66(5)	550.5(3)	10
52	7.264(3)	7.262(4)	10.428(5)	89.66(6)	550.1(4)	10
38	7.263(4)	7.260(4)	10.425(6)	89.64(6)	549.7(4)	10
24	7.244(6)	7.264(3)	10.422(4)	89.64(4)	548.5(3)	9
10	7.243(5)	7.265(2)	10.422(3)	89.64(3)	548.3(3)	9

[a] For the monoclinic structure the cell choice is given according to Brown (Ref. 2) with $\beta < 90°$.
[b] According to the calorimetric experiments, the measurements at $T = 206$ K should be of the monoclinic structure, but with $a = b$ and β very close to 90°, the diagram shows tetragonal symmetry.

determination of $(NH_4)_2SeBr_6$.[5] The legitimacy of the rigid-body model can be checked by calculating a generalized R index for the agreement of the observed and calculated U_{ij} (program XANADU[20]): $R_G = 0.032$. The root mean squared angular displacement of the libration is 5.15° off the center position. This is a rather high value, consistent with the low-temperature instability of the cubic structure. For $(NH_4)_2SeBr_6$, for example, the angular displacement is only 3.84°,[5] indicating a lower critical temperature for the first transition than in K_2SeBr_6.

The goal of the x-ray powder diffraction was to delineate polymorphism in K_2SeBr_6: the powder diffraction diagrams can be associated unambiguously with three phases. The room-temperature cubic phase transforms continuously at about 240 K (onset) into a tetragonal phase with the Rb_2TeI_6 structure (space group $P4/mnc$).[21] This structure is stable until about 200 K; below this a second-order phase transition yields a monoclinic structure (K_2TeBr_6-type; space group $P2_1/n^2$). Both these phase transitions are reversible in the x-ray powder experiment without any observed hysteresis. No further changes of the diffraction pattern were observed, indicating the stability of the $P2_1/n$ structure down to $T = 10$ K. All these features indicate that this material probably is ferroelastic.

Table III gives the lattice parameters in steps of 14 K evaluated from the least squares refinement with reflections unambiguously associated with indices hkl. Due to the very high pseudo-symmetry of the distorted structures, there are only very few reflections without any coincidences.

Figures 2 and 3 illustrate the lattice parameters as a function of temperature. The separation of the a and b axes in the monoclinic phase is not observable until very low temperature. A jump of the volume of the unit cell also is observed in this temperature range.

The experimental heat capacity results are listed in Table IV. As no sample history effects were observed, the data are given in order of increasing temperature. Relaxation

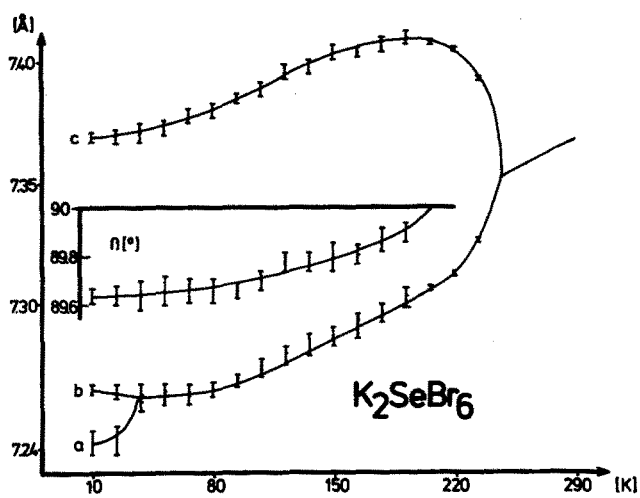

FIG. 2. The lattice parameters of K_2SeBr_6 as a function of temperature. The values of the c axis are divided by $\sqrt{2}$, as is a for the cubic phase.

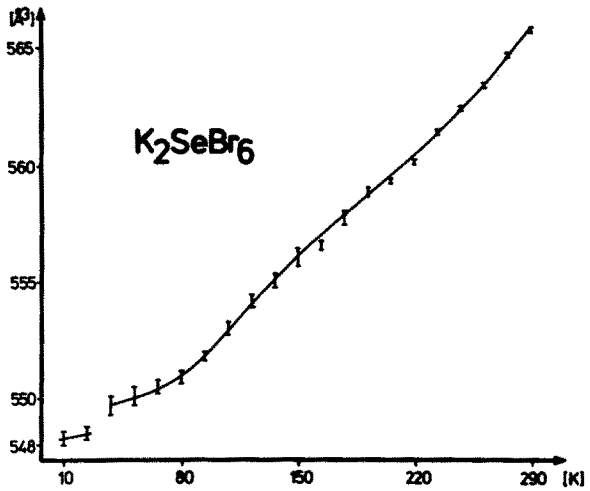

FIG. 3. The volume of the unit cell of K_2SeBr_6 (with $Z = 2$) as a function of temperature.

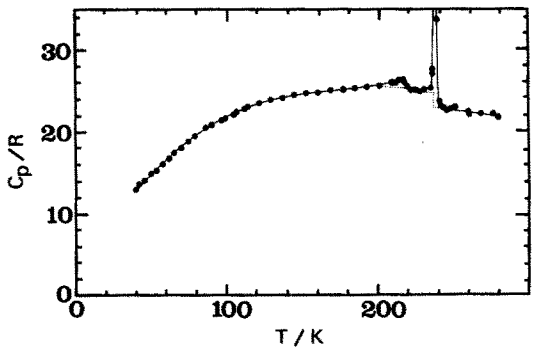

FIG. 4. The experimental heat capacity of K_2SeBr_6 as a function of temperature. The broken lines represent the "base line" heat capacities used for the evaluation of the thermodynamics of the phase changes.

times following the introduction of a heat pulse were of the order of a few minutes, i.e., in the normal range for this calorimeter. (Longer relaxation times can be indicative of unusual thermal effects.[22]) Figure 4 shows the experimental heat capacity of K_2SeBr_6 as a function of temperature.

IV. DISCUSSION

Several features are apparent immediately from the heat capacity results of Fig. 4, viz.: the thermal anomalies at ~215 K and at ~238 K, and the rapid decrease in the base line heat capacity from below this anomalous temperature region to above it. Although the calorimetric features near 215 and 238 K are undoubtedly related to the phase transformations in K_2SeBr_6, and therefore pertinent, we defer their discussion until later in this paper, and turn our attention now to the base line heat capacity.

The heat capacities that are measured in our sealed calorimeter are truly C_s values, i.e., the heat capacities of the solid in equilibrium with its saturated vapor. C_s is related to C_p, the heat capacity at constant pressure by[23]:

$$C_s - C_p = \left(\frac{\partial P}{\partial T}\right)_{\text{sat}} \left[\left(\frac{\partial H}{\partial P}\right)_T - V\right]. \tag{1}$$

In the temperature range of these calorimetric experiments, the vapor pressure of K_2SeBr_6 is extremely low, and the difference between C_s and C_p will be negligible. C_p and C_v, the heat capacity at constant volume, are related by[23]

$$C_p - C_v = \alpha^2 VT/\kappa_T, \tag{2}$$

where V is the molar volume, α is the coefficient for cubic thermal expansion ($= V^{-1} dV/dT$), and κ_T is the isothermal compressibility. Equation (2) strictly applies only to the case of a cubic lattice. While it is used commonly for noncubic lattices, this is reasonable only in the case of nearly isotropic thermal expansion. In the case of anisotropic thermal expansion, especially where the linear thermal expansion is negative in one direction and the bulk thermal expansion is positive, as we see here for K_2SeBr_6 (Table V, derived from the data of Table I), a more detailed approach is required.

TABLE IV. The experimental molar heat capacity of K_2SeBr_6. $R = 8.31451\ \text{J K}^{-1}\ \text{mol}^{-1}$.

T/K	C_p/R	T/K	C_p/R	T/K	C_p/R
39.41	13.05	168.43	25.22	241.87	23.06
42.32	13.80	176.45	25.29	242.71	23.24
45.70	14.19	184.51	25.50	245.15	22.77
49.92	15.11	192.62	25.60	247.60	22.86
53.50	15.46	200.80	25.68	249.93	23.13
57.04	16.11	208.67	26.08	250.66	23.07
61.16	16.82	209.01	26.09	259.09	22.60
65.29	17.49	211.46	26.06	259.48	22.35
69.19	18.14	214.19	26.50	267.54	22.33
73.04	18.61	216.90	26.56	275.65	22.33
76.88	19.24	217.25	26.22	278.99	21.92
86.02	20.68	219.65	25.63		
90.27	21.02	222.40	25.22		
96.56	21.64	225.16	25.32		
98.69	21.79	225.58	25.21		
104.14	22.32	227.90	25.06		
106.23	22.59	230.65	25.25		
111.74	22.99	234.69	25.46		
113.79	23.25	235.58	27.18		
121.40	23.70	236.04	27.68		
129.08	24.05	237.15	42.90		
136.85	24.28	237.85	51.26		
144.66	24.63	238.64	33.85		
152.54	24.85	240.25	23.90		
160.45	24.95	241.29	23.16		

TABLE V. The coefficients of thermal expansion of K_2SeBr_6 at selected temperatures. In the monoclinic phase ($T < 215$ K), α_a and α_b are too similar to be distinguished.

T/K	α_a/K^{-1}	α_c/K^{-1}
100	5×10^{-5}	3×10^{-5}
150	5×10^{-5}	5×10^{-5}
180	5×10^{-5}	3×10^{-5}
200	5×10^{-5}	0
220	7×10^{-5}	-5×10^{-5}
230	1.7×10^{-4}	-1.3×10^{-4}
235	2.5×10^{-4}	-7×10^{-4}
240	4.8×10^{-5}	4.8×10^{-5}
280	4.8×10^{-5}	4.8×10^{-5}

Of particular initial interest is the general *decrease* in the heat capacity (aside from the phase transitions) with increasing temperature above about 220 K. In light of the negative thermal expansion along the c axis and the finding that negative thermal expansion is responsible for much of the anomalous heat capacity in some ammonium salts,[24] we chose to examine in some detail the contribution of $p - V$ work to the heat capacity.

Above 238 K, K_2SeBr_6 is cubic, and C_e, the heat capacity at constant strain, can be evaluated from the following relationship[24]:

$$C_p - C_e = 3VT\alpha^2(c_{11} + 2c_{12} + c_{44}), \tag{3}$$

where C_p is the experimental heat capacity, V is the molar volume, and α is our measured cubic thermal expansion, T is the temperature, and c_{ij} are elastic constants as measured at room temperature for K_2SeBr_6 by Wruk *et al.*[25]

From 215 to 238 K, K_2SeBr_6 is tetragonal and C_e is given by[24]

$$C_p - C_e = VT\left[2(c_{11} + c_{12})\alpha_a^2 + 4c_{13}\alpha_a\alpha_c + c_{33}\alpha_c^2\right], \tag{4}$$

where α_a and α_c are the measured coefficients of thermal expansion along the a and c axes, respectively ($\alpha_i = x^{-1}\, dx/dT, x = a,c$). There are no published values of the elastic constants of K_2SeBr_6 in this temperature range; we return to this point later.

Below 215 K, K_2SeBr_6 is monoclinic, but sufficiently close to tetragonal that we will make use of Eq. (4) to evaluate C_e, especially since again we do not have experimental elastic constant data in this temperature range.

As an answer to the question of whether the general decrease in C_p is related to $p - V$ work in the thermal evolution of the lattice, we present Fig. 5 which shows C_p and also C_e calculated from Eqs. (3) and (4). As discussed above, for $T > 238$ K, C_e is fully determined from experimental data. Below 206 K there is an uncertainty in the values of the elastic constants, so we have chosen to examine several models. If the common elastic constants below 206 K are taken to be the same as at room temperature, and c_{13} and c_{33} at the lower temperatures are taken to equal the room-temperature c_{44} value, this gives the "K_2SeBr_6 room-temperature-modified" curve for C_e shown in Fig. 5. A reduction of c_{13} and c_{33} by a factor of 2 increases C_e by less than 1%. It is clear that in neither of these models is $p - V$ work sufficient to account for the unusual temperature evolution of the observed heat capacity.

Of course, if the lattice was stiffer below 206 K than at room temperature, this would reduce C_e considerably. For example, increasing all the values of the elastic constants by about 50% in Eq. (4) yields the "stiffer lattice" curve shown in Fig. 5. This curve still shows C_e at, for example, 190 K to greatly exceed that above 240 K. The answer to our question—Is the anomalously high heat capacity just below 200 K due to unusual $p - V$ contributions?—appears to be in the affirmative only if the lattice is extraordinarily stiff at low temperatures.

Again, since we have accurate thermal expansion data for K_2SeBr_6 and despite the absence of elastic constant data for this salt in this temperature range, we thought it worth exploring the contribution of $p - V$ work to the anomalous heat capacity in the temperature range of the 215 K anomaly especially since this coincides with the temperature range of negative thermal expansion along the c axis. We have used Eq. (4) and the temperature-independent K_2SeBr_6 room-temperature-modified elastic constants (as described above) to calculate the heat capacity at constant strain C_e. The results of this calculation are shown in Fig. 6, and again a reduction of c_{13} and c_{33} by a factor of 2 makes little difference. Included for comparison in Fig. 6 are the C_e results for a stiffer lattice, as described above. It is apparent from this figure that the source of the anomaly around 215 K is not the negative thermal expansion along the c axis.

Turning now to the matter of the phase transitions in K_2SeBr_6, we note the two anomalies in the experimental heat capacity data shown in Fig. 4.

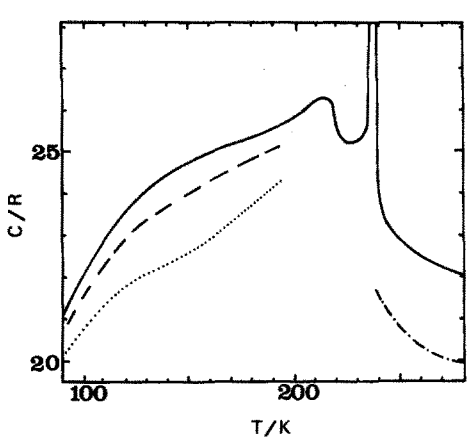

FIG. 5. The experimental heat capacity (solid line), and calculated heat capacity at constant strain (C_e) for K_2SeBr_6 as a function of temperature. The dashed line is C_e from the "K_2SeBr_6 room-temperature-modified" model, as described in the text, and the dotted line is C_e for the "stiffer lattice" model, as described in the text. At higher temperatures, C_e (dot–dash line) is calculated from Eq. (6) as described in the text.

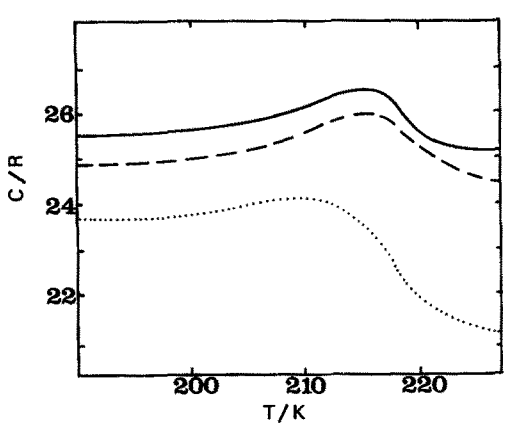

FIG. 6. The experimental heat capacity (solid line), and two models of the heat capacity at constant strain (C_e) for K_2SeBr_6 as a function of temperature in the region of the lower-temperature phase transition. The dashed line is C_e for the K_2SeBr_6 room-temperature-modified model, as described in the text, and the dotted line is C_e for the stiffer lattice model, as described in the text.

TABLE VI. The thermodynamic changes associated with the phase transitions in K_2SeBr_6. $R = 8.314\,51\ J\ K^{-1}\ mol^{-1}$.

Space group change	T_{tr}/K	ΔH_{tr}/ (J mol^{-1})	ΔS_{tr}/R
$Fm\bar{3}m \rightarrow P4/mnc$	237.8 ± 0.3	325 ± 6	0.164 ± 0.002
$P4/mnc \rightarrow P2_1/n$	215 ± 1	162 ± 6	0.0955 ± 0.0035

The higher-temperature anomaly has its heat capacity maximum at 237.8 ± 0.8 K. Its source is the $Fm\bar{3}m \rightarrow P4/mnc$ phase transformation, possibly with a slight first-order character, as seen calorimetrically. Because of the other anomalous aspects of the heat capacity near this transformation, it is difficult to accurately delineate the excess heat capacity from the background. However, taking the background heat capacity as that shown by a dashed line in Fig. 4, we have assessed the thermodynamic changes associated with this phase transition. These data are summarized in Table VI.

The lower-temperature heat capacity anomaly has a maximum at 215 ± 1 K. If we consider the base line heat capacity in this temperature region to be linear and to meet with the experimental data at 190 and 228 K, as shown by the dashed line in Fig. 4, this yields the phase transition data given in Table VI.

We can compare our phase transition determinations with earlier literature for K_2SeBr_6. An NQR study[10] showed phase transitions at 240, 221, and 209 K. We can see now from our calorimetric results that the first of these corresponds to our high-temperature transition, and the latter two temperatures correspond to the onset and termination of the lower-temperature transition, respectively. This transition has no first-order character; in higher-order transitions it is not unprecedented for a microscopic probe to detect changes at temperatures other than the maximum in the heat capacity anomaly.[26]

The only other further evidence of the phase transitions in K_2SeBr_6 appears to be the x-ray study and neutron scattering studies of Noda *et al.*[11,27] Their data agree with the NQR phase transition temperatures; we believe that these

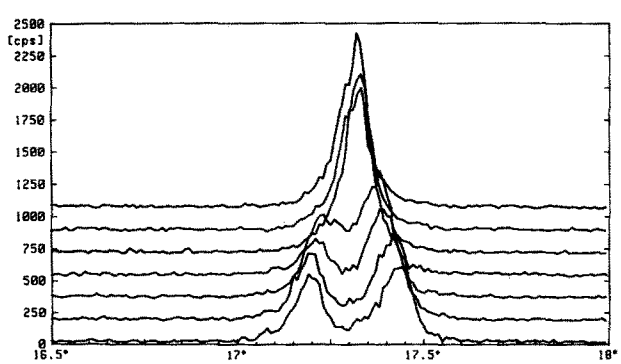

FIG. 7. θ scan multidisplay (CuKα_1 radiation) of a characteristic section of the diffraction patterns. Splitting of the cubic 440 reflection (top) yields tetragonal reflections 004 and 220 (bottom scan). The diagrams are recorded in temperature steps of -5 K, starting at $T = 255$ K (top).

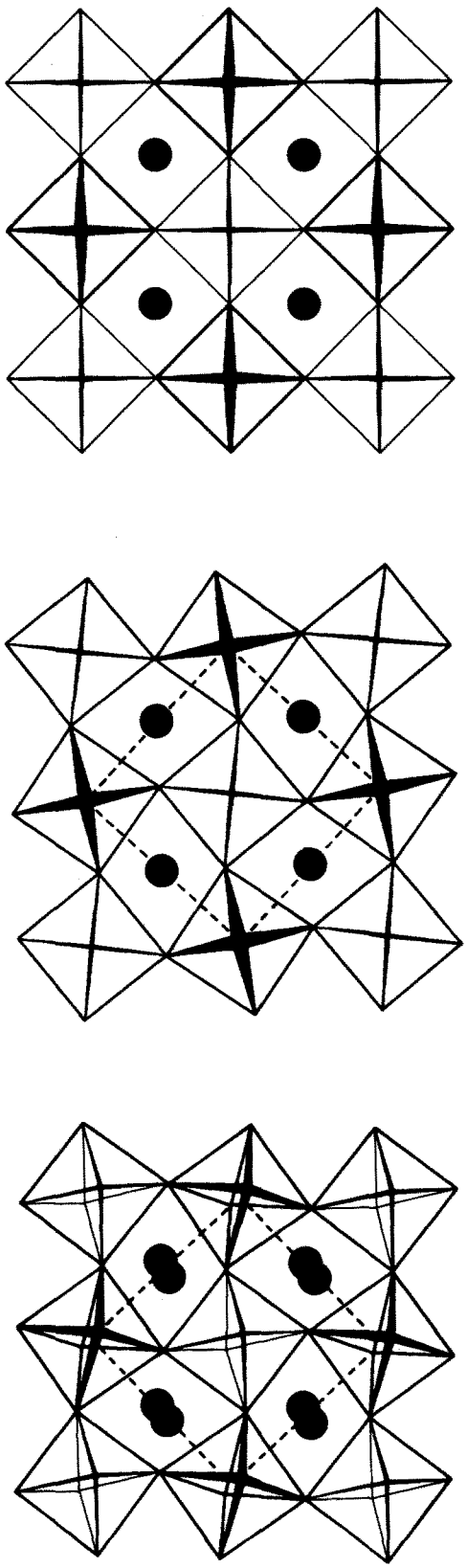

FIG. 8. The structures of the high- and low-temperature polymorphs of K_2SeBr_6, projected along the c axis: (a) cubic K_2PtCl_6-type structure, space group $Fm\bar{3}m$ with $Z = 4$; (b) tetragonal Rb_2TeI_6-type structure, space group $P4/mnc$ with $Z = 2$ (antiferrorotative distortion); (c) monoclinic K_2TeBr_6-type structure, space group $P2_1/n$ with $Z = 2$ (antiferrorotative distortion, additional tilt against [001]). Different heights of $SeBr_6^{2-}$ octahedra are given by different line thicknesses (thin: $z = 0$; thick: $z = 1/2$); K^+ at $z = 1/4$ and $z = 3/4$.

authors have been unduly influenced by the previously published NQR data, as the only evidence that Noda *et al.* present for the extra transition is the variation in the intensity of one superlattice reflection which, according to their Fig. 3 in Ref. 11, is within background intensity. Furthermore, cooling down single crystals below the temperature of a phase transition usually gives rise to twinning (for the transition $Fm\bar{3}m \rightarrow P4/mnc$ one observes triplet crystals due to the loss of the threefold axis), yet Noda *et al.*[11] do not report this for their single crystal results. A very careful check of our powder diagrams in the critical temperature range between 250 and 190 K only showed the transitions at 238 and 215 K. As an example, the splitting of the cubic 400 reflection is shown in Fig. 7. (This figure also shows the resolution of the x-ray powder diffraction experiment.) Noda *et al.* also show a phase transition at 160 K, but we see no evidence of this in either our calorimetric or x-ray diffraction data.

Figure 8 gives projection views of the corresponding structure types in all three phases of K_2SeBr_6.

The transitional entropy changes for both phase changes are so small as to make $R \ln \omega$ interpretation meaningless (ω would be 1.2 and 1.1 for the high- and low- temperature transitions, respectively). Therefore, the transitions, based on calorimetric evidence, are not related to order–disorder, but rather to more subtle effects. The phase transition that we observe at 215 K ($P4/mnc \rightarrow P2_1/n$) has all the markings of a soft mode transition,[28] viz. a small entropy change, and a transition over a wide temperature range ($\sim$20 K) with finite heat capacity throughout. The phase transition at 238 K seems to be predominantly second-order, too, considering the x-ray diffraction data (continuous change of diffraction pattern, no hysteresis). With two transitions of second order, the behavior of K_2SeBr_6 could be consistent with diffraction results for K_2TeBr_6.[29–32] For both compounds the phase transitions should arise from the softening of rotational phonons. From the group–subgroup relations of the corresponding space groups,[10] the softening phonons can be denoted according to Sutton and Armstrong.[33,34] Both transitions take place at the X edge of the cubic F-centered Brillouin zone: the $A_{2g}(X)$ rotary phonon for $Fm\bar{3} \rightarrow P4/mnc$; the $E_g(X)$ rotary phonon for $P4/mnc \rightarrow P2_1/n$. (For a more detailed discussion see, for example, recent papers by Abrahams and Ihringer.[32,35])

Finally, the phase transitions give rise to a more condensed packing by an antiferrorotative displacement of the $SeBr_6^{2-}$ octahedra. From Landau's theory, the order parameter for these necessarily second-order transitions could be the squared frequency of the softening phonons or the squared tilt angle of the octahedral displacement. All these features are significant for a ferroelastic material, and worthy of further investigation.

ACKNOWLEDGMENTS

The authors thank J. Leiper for assistance. Financial support from the Deutsche Forschungsgemeinschaft and the Fonds der Chemischen Industrie (to W.A.), the Natural Sciences and Engineering Research Council of Canada (to M.A.W.) is gratefully acknowledged. Both authors thank NATO for a Collaborative Research Grant.

[1] R. J. Gillespie and R. S. Nyholm, Q. Rev. Chem. Soc. **11**, 339 (1957).
[2] I. D. Brown, Can. J. Chem. **42**, 2758 (1964).
[3] R. J. Gillespie, *Molecular Geometry* (Van Nostrand Reinhold, London, 1972).
[4] W. Abriel, Acta Crystallogr. B **42**, 449 (1986).
[5] W. Abriel, Z. Naturforsch. Teil B **42**, 415 (1987).
[6] W. Abriel and E. -J. Zehnder, Z. Naturforsch. Teil B **42**, 1273 (1987).
[7] W. Abriel, Acta Crystallogr. C **42**, 1113 (1986).
[8] W. Abriel and A. du Bois, Z. Naturforsch. Teil B **44**, 1187 (1989).
[9] J. Ihringer, Acta Crystallogr. A **36**, 89 (1980).
[10] D. Nakamura, K. Ito, and M. Kubo, Inorg. Chem. **2**, 61 (1963).
[11] Y. Noda, T. Ishii, M. Mori, and Y. Yamada, J. Phys. Soc. Jpn. **48**, 1279 (1980).
[12] J. L. Hoard and B. N. Dickinson, Z. Kristallogr. **84**, 436 (1933).
[13] International Union of Crystallography, Acta Crystallogr. B **38**, 699 (1982).
[14] *International Tables for X-Ray Crystallography, Vol. IV* (Kynoch, Birmingham, 1974). Present distributor: Reidel, Dordrecht. See also material deposited in PAPS. See AIP document No. PAPS JCPSA-93-8321-03 for 3 pages of lists Order by PAPS number and journal reference from American Institute of Physics, Physics Auxiliary Publication Service, 335 East 45th Street, New York, NY 10017. The price is $1.50 for each microfiche (98 pages) or $5.00 for photocopies of up to 30 pages, and $0.15 for each additional page over 30 pages. Airmail additional. Make checks payable to the American Institute of Physics.
[15] W. Abriel and U. Bismayer, Phase Trans. **15**, 49 (1989).
[16] M. A. White, Thermochimica Acta **74**, 55 (1984).
[17] M. J. M. Van Oort and M. A. White, Rev. Sci. Instrum. **58**, 1239 (1987).
[18] D. C. Ginnings and G. T. Furukawa, J. Am. Chem. Soc. **75**, 522 (1953).
[19] B. T. M. Willis and A. W. Pryor, *Thermal Vibrations in Crystallography* (Cambridge University, London, 1975).
[20] P. Roberts and G. M. Sheldrick, XANADU, unpublished program (1975).
[21] W. Abriel, Mater. Res. Bull. **17**, 1341 (1982).
[22] M. A. White, C. Chieh, A. Anderson, and L. A. K. Staveley, J. Chem. Phys. **80**, 1254 (1984).
[23] J. G. Aston and J. J. Fritz, in *Thermodynamics and Statistical Thermodynamics* (Wiley, New York, 1959).
[24] R. J. C. Brown, J. E. Callanan, R. D. Weir, and E. F. Westrum, Jr., J. Chem. Phys. **85**, 5963 (1986); **86**, (E) 3759 (1987).
[25] N. Wruk, J. Pelzl, G. A. Saunders, and Tu Hailing, J. Phys. Chem. Solids **46**, 1235 (1985).
[26] M. A. White and A. Perrott, Can. J. Chem. **66**, 729 (1988).
[27] Y. Noda, N. Iizumi, and Y. Yamada, JAERI-M-8009, Annu. Rep. Neutron. Scatt. Stud., 19 (1978).
[28] H. Chihara, Ber. Bunsenges. Phys. Chem. **87**, 188 (1983).
[29] W. Abriel, Mater. Res. Bull. **18**, 1419 (1983).
[30] W. Abriel, Mater. Res. Bull. **19**, 313 (1984).
[31] S. C. Abrahams, J. Ihringer, P. Marsh, and K. Nassau, J. Chem. Phys. **81**, 2082 (1984).
[32] S. C. Abrahams, J. Ihringer, and P. Marsh, Acta Crystallogr. B **45**, 26 (1989).
[33] M. Sutton and R. L. Armstrong, Phys. Rev. B **25**, 1813 (1982).
[34] M. Sutton and R. L. Armstrong, Phys. Rev. B **27**, 1937 (1983).
[35] J. Ihringer and S. C. Abrahams, Phys. Rev. B **30**, 6540 (1984).